Supporting Information

Mellado Lagarde et al. 10.1073/pnas.1408064111

SI Materials and Methods

Mouse Models. Ai14:Rosa26^{tdTom} mice have a CAG promoter-driven red fluorescent protein variant (tdTomato, called here "Tomato"), which is expressed after removal of a loxP-flanked stop cassette knocked in the Rosa26 locus and serve as a high-efficiency reporter of Cre activity (1). Rosa26^{DTA} transgenic mice of both genders (2) were purchased from The Jackson Laboratory (stock no. 006331) and genotyped using primers recognizing the DTA sequence (5′-TGACGATGATTGGAA-AGGGT-3′ and 5′-TGAGCACTACACGCGAAGCA-3′) that generated a 300-bp band showing presence of the DTA allele. The Pou4f3CreER^{T} mouse line (3) was generated by placing the Pou4f3 (Brn3.1) regulatory sequence (4) upstream of the CreER^{T} coding sequence (5).

PlpCreER^{T};Rosa26^{DTA} (PlpDTA) mice of either sex were induced with tamoxifen (Sigma T5648-5G diluted in corn oil at 37 °C; Sigma C8267) once each day at P0 and P1 at doses of 0.05–0.075 mg/g bodyweight (i.p. injection at room temperature) and were studied at ages P5 to 7 wk in comparison with control mice of either sex and of the same age. Leucine-rich repeat-containing G-protein coupled receptor 5 (Lgr5)CreER^{T2}; Rosa26^{DTA} (Lgr5DTA) and glutamate aspartate transporter (Glast)CreER^{T};Rosa26^{DTA} (GlastDTA) mice of either sex were induced similarly with tamoxifen at P0 and P1. Lgr5DTA mice and their control littermates all carry a single β-catenin loss-of-function floxed allele (The Jackson Laboratory, stock no. 004152) that has no impact on cochlear morphology or function, as expected from the absence of phenotype described in heterozygous of germline knockout mice (6). GlastDTA mice were also induced with tamoxifen once each day at P15 and P16 (0.075 mg/g bodyweight, i.p.) or once at P21 (0.225 mg/g bodyweight, i.p.) and were studied 3 wk later at P37 or P41, respectively. Littermates of either sex with only one of the mutant genes (i.e., CreER^{T} or Rosa26^{DTA}) were used as controls and were induced with tamoxifen identically to experimental mice. Genotyping and tamoxifen-induction protocols have been described previously (7–10).

Immunohistochemistry. Inner ears were dissected out of the temporal bone and fixed in 4% paraformaldehyde in 10 mM PBS (pH 7.4) for 15–20 min at room temperature or overnight at room temperature. Inner ears from P10 or older mice were decalcified with 120 mM EDTA in 10 mM PBS (pH 7.4) at 4 °C. For whole mounts, cochleae were dissected and divided into two or three pieces.

Sections and whole mounts were washed with 10 mM PBS and blocked with 1% BSA, 10% goat or horse serum, and 1% Triton X-100 in PBS for 1 h at room temperature. Primary antibodies were diluted in 1% BSA, 5% goat or horse serum, and 0.1% Triton X-100 in PBS and were incubated overnight at 4 °C. Appropriate secondary Alexa-conjugated antibodies (1:1,000; Life Technologies), diluted in 1% BSA, 5% normal goat or horse serum, and 0.1% Triton X-100 in PBS, were incubated for 1–2 h at room temperature. PBS washes were performed between steps during the immunostaining protocol. For analysis of Tomato^{+} or eGFP^{+} samples, endogenous fluorescence was measured. Primary antibodies used were rabbit anti-MyosinVIIa (Myo7a, 1:200; Proteus Biosciences), mouse anti-parvalbumin (1:1,000; Sigma), goat anti-Sox2 (1:500; Santa Cruz Biotechnology), rabbit anti-GLAST (1:100; from Abcam or a gift from Niels C. Danbolt, University of Oslo, Oslo), mouse anti-Ctbp2 (1:100; BD Transduction Laboratories), mouse anti-GluR2 (1:200; Millipore), and mouse anti-Tuj1 (1:500; Covance). Nuclei were labeled with Hoechst 33342 (1:2,000; Life Technologies) or DAPI (1:2,000; Life Technologies). Fluorescent images were acquired using Zeiss LSM 700 or 710 confocal microscopes. Zen 2009/2011 software was used for image acquisition. LSM Image Browser and Adobe Photoshop CS5 were used for image processing. ImageJ 1.46r was used for 3D reconstructions of *z*-stacks.

Counts of Cells and Subcellular Organelles. For cell counts in whole-mount images the total cochlea length was calculated in acquired low-resolution images (average value, 6,000 μm). Apex, middle, and base higher-resolution confocal images (40× objective, 160-μm region) were taken at 25%, 50%, and 75% of the cochlear length from the apical tip, respectively. SCs were identified by their location relative to IHCs and OHCs and the expression of the Sox2 marker in *z*-stacks of the organ of Corti. Specifically, for IBC/IPhC counts at earlier ages (P5–8), only Sox2^{+} nuclei lying in close contact with the IHC and IPC nuclei were considered, avoiding errors arising from the inclusion of neighboring GER cells (Fig. S2*B*). In mice age P15 and older, all Sox2^{+} nuclei remaining close to the IHCs were considered on the counts, because the GER has already receded at these ages (Fig. S2*B*). It is important to note that IPC nuclei (which also are Sox2^{+}) are clearly differentiated from IBCs/IPCs by their location, limiting the medial edge of the tunnel of Corti, and clear longitudinal organization.

For quantification of GER cells, Tomato^{+} or Sox2^{+} nuclei were counted in optical sections (indicated as "OS" in graphs) extracted from *z*-stack confocal images (Fig. S5 *A* and *D*). Three different, randomly selected optical sections were used from each 160-μm region imaged, and counts were averaged per mouse before the averaging of individuals in the control and experimental groups.

For counts of synaptic buttons at individual cochlear frequencies, all pieces of each cochlea were imaged at low magnification to convert cochlear locations to frequency using a custom ImageJ plugin (www.masseyeandear.org/research/otolaryngology/investigators/laboratories/eaton-peabody-laboratories/epl-histology-resources/imagej-plugin-for-cochlear-frequency-mapping-in-whole-mounts/).

ABR. Mice 4 wk old and older were anesthetized with avertin (2,2,2 tribromoethanol, Sigma) (0.6 mg/g body weight, i.p.) and were kept on a heating pad at 37 °C. ABRs were measured using a TDT System III with RZ6 multiprocessors and BioSigRZ software (Tucker Davis Technologies). Tone signals were calibrated using a 0.25-in PCB microphone (PCB-FF-1/4) connected to the RZ6 multiprocessor analog/digital input. Calibrated and attenuated sinusoidal signals (0.5-ms rise time, 5-ms duration) were fed into an MF-1 magnetic speaker (Tucker Davis Technologies) using the digital/analog output of the multiprocessor (200-kHz sampling rate). The MF-1 magnetic speaker was placed 5 cm in front of the mouse's left ear, where the reference electrode was located. Frequencies tested were 4, 6, 12, 16, 22, 32, and 44 kHz with sound pressure level (dB SPL, relative to 20 μPa) attenuated in 5-dB steps between 70 and 0 dB SPL or higher levels if hearing loss was present. ABR waveforms were recorded using subdermal needles placed at the vertex of the skull, below the pinna, and at the base of the tail. The needles were connected to a low-impedance head-stage (RA4LI; Tucker Davis Technologies) and fed into the optical port of the RZ6 multiprocessor through a preamplifier (RA4PA, gain 20×;

Tucker Davis Technologies). ABR waveforms were averages obtained from 500 presentations of the tone (21/s) in alternating phase and were band-pass filtered (300 Hz–3 kHz). Thresholds in the ABR tuning curves were defined as the minimum dB SPL of a tone that elicited a wave I above the noise floor. All experiments were conducted in a sound booth (Industrial Acoustic Company Model 120A double wall). ABR thresholds were plotted using Origin 9.0 software.

Cell Proliferation Studies. Cell proliferation at different times after tamoxifen induction was studied in PlpDTA and control mice using i.p. injections at different ages of one of the nucleoside analogs of thymidine (BrdU, 15 μL/g bodyweight of a 10-mM solution from Roche) or EdU (10 μg/g bodyweight of a 10-mM solution provided with the Click-iT EdU Imaging Kit from Life Technologies). These nucleoside analogs are incorporated into the DNA during active DNA synthesis. EdU staining was performed using the Click-iT EdU imaging kit (Life Technologies) following the manufacturer's instructions. BrdU staining requires a previous step of acid treatment of the tissue with 2N HCl for 25 min at 37 °C followed by washes with 0.1 M Tris·HCl (pH 8.0). For BrdU labeling an anti-BrdU Alexa 488-conjugated antibody was used (1:20 dilution; Life Technologies).

1. Madisen L, et al. (2010) A robust and high-throughput Cre reporting and characterization system for the whole mouse brain. *Nat Neurosci* 13(1):133–140.
2. Ivanova A, et al. (2005) In vivo genetic ablation by Cre-mediated expression of diphtheria toxin fragment A. *Genesis* 43(3):129–135.
3. Wan G, Gomez-Casati ME, Gigliello AR, Liberman C, Corfas G (2014) Neurotrophin-3 regulates ribbon synapse density in the cochlea and induces synapse regeneration after acoustic trauma. *eLife*, 10.7554/eLife.03564.
4. Sage C, et al. (2006) Essential role of retinoblastoma protein in mammalian hair cell development and hearing. *Proc Natl Acad Sci USA* 103(19):7345–7350.
5. Feil R, et al. (1996) Ligand-activated site-specific recombination in mice. *Proc Natl Acad Sci USA* 93(20):10887–10890.
6. Haegel H, et al. (1995) Lack of beta-catenin affects mouse development at gastrulation. *Development* 121(11):3529–3537.
7. Fang J, et al. (2012) Outer hair cell-specific prestin-CreERT2 knockin mouse lines. *Genesis* 50(2):124–131.
8. Chai R, et al. (2012) Wnt signaling induces proliferation of sensory precursors in the postnatal mouse cochlea. *Proc Natl Acad Sci USA* 109(21):8167–8172.
9. de Melo J, et al. (2012) Injury-independent induction of reactive gliosis in retina by loss of function of the LIM homeodomain transcription factor Lhx2. *Proc Natl Acad Sci USA* 109(12):4657–4662.
10. Wang Y, et al. (2012) Norrin/Frizzled4 signaling in retinal vascular development and blood brain barrier plasticity. *Cell* 151(6):1332–1344.

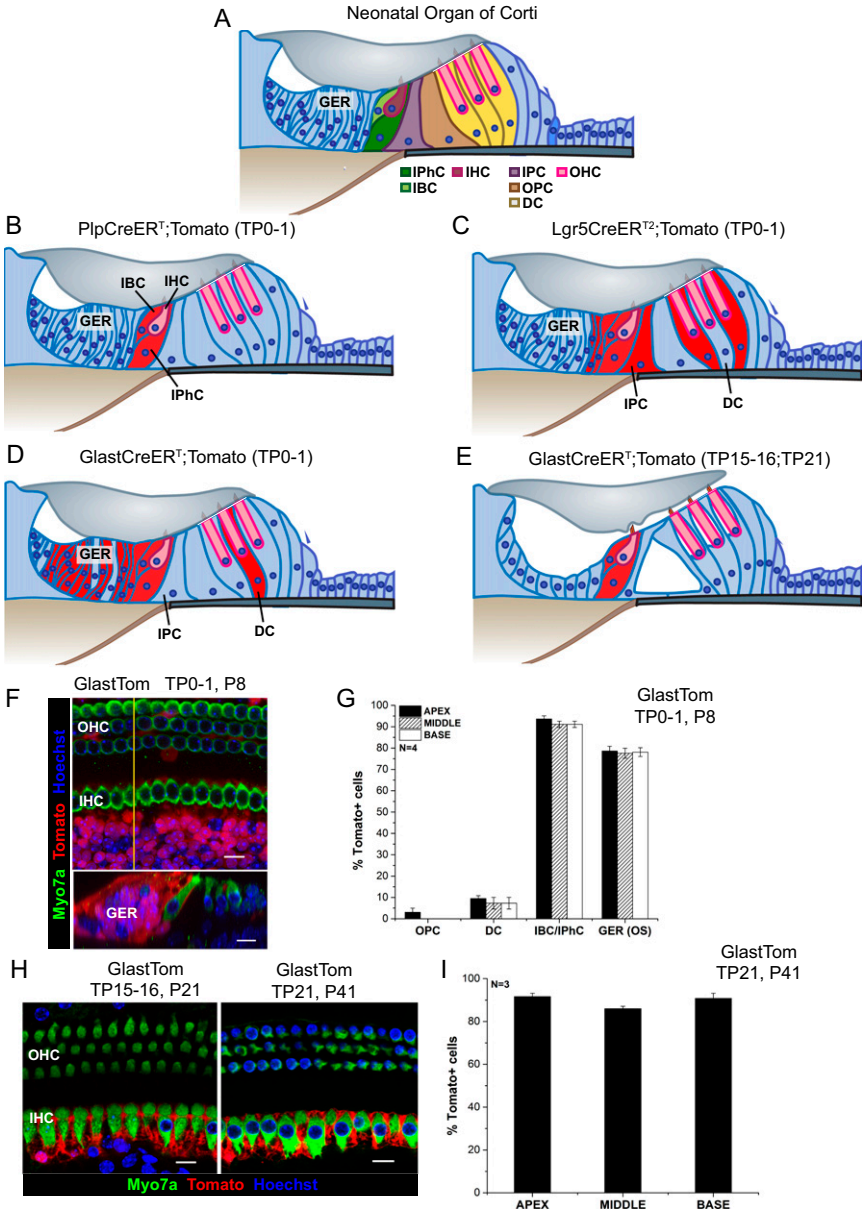

Fig. S1. Cell specificity of CreER^{T} lines in the organ of Corti reported by Ai14:Rosa26^{tdTom} (Tomato) reporter. (*A*) Scheme of a section of the neonatal organ of Corti showing different cell types present. DC, Deiters cell; GER, greater epithelial ridge cell; IBC, inner border cell; IHC, inner hair cell; IPC, inner pillar cell; IPhC, inner phalangeal cell; OHC, outer hair cell; OPC, outer pillar cell. (*B–D*) Schemes of sections of the neonatal organ of Corti in mice and representations of cells labeled with Tomato after tamoxifen induction at P0 and P1 (TP0–1) for PlpCreER^{T} (*B*), Lgr5CreER^{T2}(*C*), and GlastCreER^{T} (*D*). (*E*) Scheme of a section of the juvenile/adult organ of Corti in GlastCreER^{T} mice and representation of cells labeled with Tomato after tamoxifen induction at P15 and 16 (P15–16) or P21. HCs are shown in pink, and SCs that show Cre recombination with each CreER^{T} are shown in red. (*F*, *Upper*) Representative optical section of the apical turn of the organ of Corti of GlastTom mice induced with tamoxifen at P0 and P1; cochleae were analyzed at P8. (*Lower*) Optical cross-section extracted from *z*-stack. The position of the section is indicated by the yellow line in the upper panel. (*G*) Quantification of percentage of Tomato^{+} SCs in apex, middle, and base of the cochleae of GlastTom mice induced with tamoxifen at P0 and P1 and analyzed at P8 (mean ± SEM, $n = 4$). GER (OS), cells of the greater epithelial ridge quantified in optical cross-sections. (*H*) Representative optical sections of the apical turn of the organ of Corti of GlastTom mice induced with tamoxifen at P15 and 16 (cochleae were analyzed at P21) (*Left*) and in mice induced with tamoxifen at P21 (cochleae were analyzed at P41) (*Right*). (*I*) Quantification of percentage of Tomato^{+} IBCs and IPhCs in apex, middle, and base of the cochleae of GlastTom mice induced with tamoxifen at P21; cochleae were analyzed at P41 (mean ± SEM, $n = 3$). (Scale bars: 10 um.)

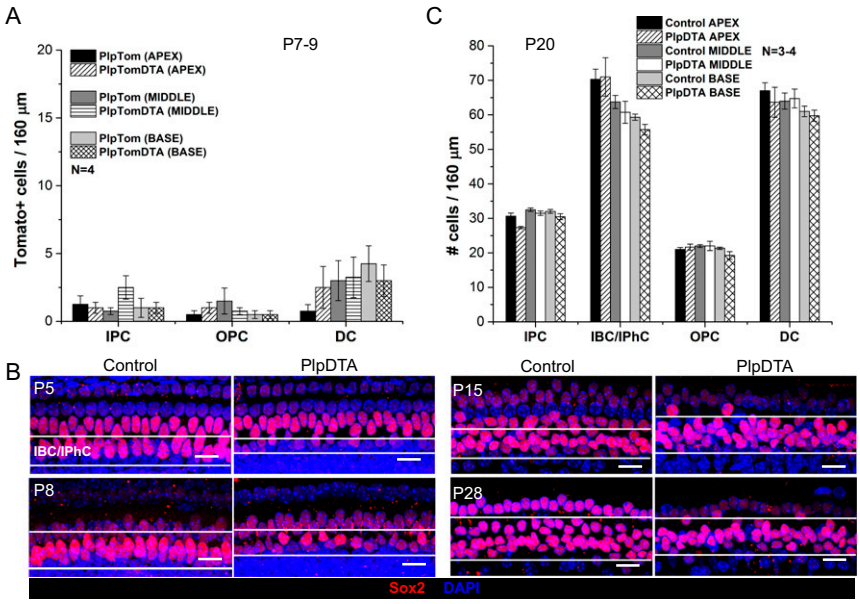

Fig. S2. Only IBCs/IPhCs are depleted in the cochleae of PlpDTA mice, and repopulation occurs in all cochlear turns. (*A*) Quantification of total number of Tomato$^+$ SCs in 160-µm regions of each turn of the cochleae of P7–9 PlpTom and PlpTomDTA mice (mean ± SEM, $n = 4$). DC, Deiters' cells; IPC, inner pillar cells; OPC, outer pillar cells. (*B*) Representative optical sections of whole mounts from the organ of Corti of PlpDTA and control mice induced with tamoxifen at P0 and P1; cochleae were collected at P5, P8, P15, and P28. Sox2$^+$ SCs are labeled in red, and DAPI$^+$ nuclei are labeled in blue. White lines show the regions where IBC/IPhC Sox2$^+$ nuclei were counted for the graphs in *A* and *C* in this figure and in Fig. 1*C*. (*C*) Quantification of total number of Sox2$^+$ SCs in 160-µm regions of each turn of the cochleae of P20 PlpDTA and control mice (mean ± SEM, $n = 3$–4). (Scale bars: 10 um.)

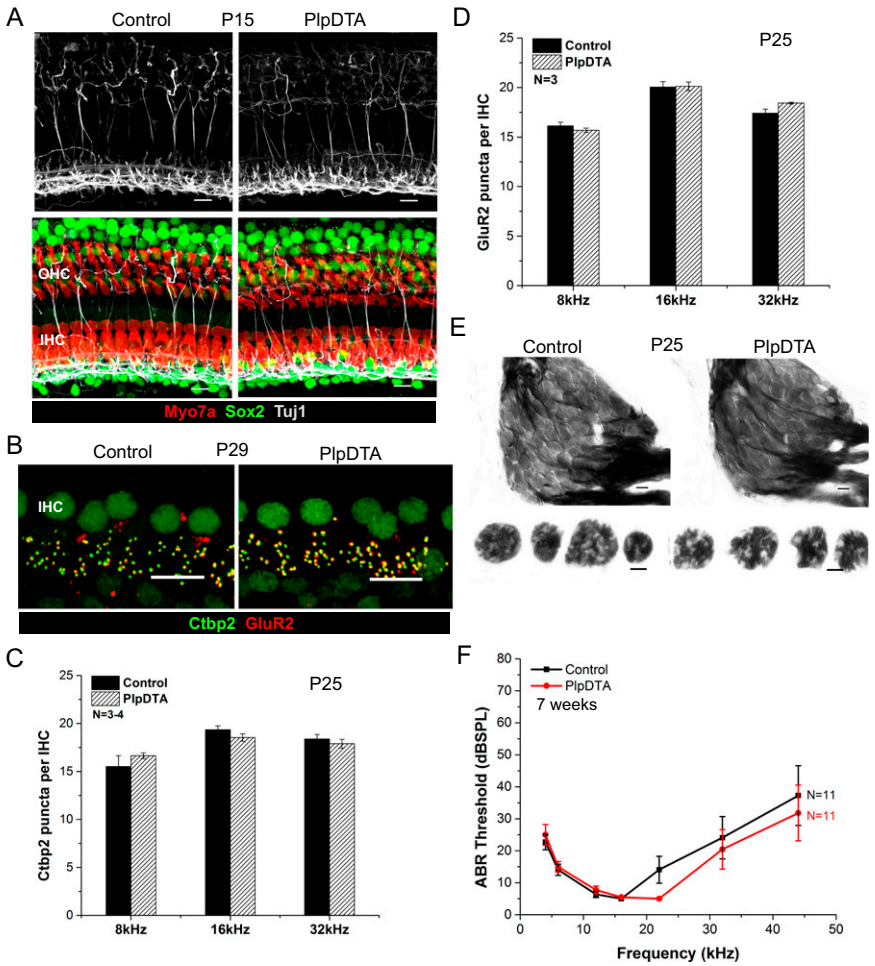

Fig. S3. IBC/IPhC ablation and repopulation does not affect neuronal survival, afferent innervation, and hearing sensitivity in PlpDTA mice. (*A*) Representative optical projections of whole mounts from the apical turn of the cochleae of P15 PlpDTA and control mice. (*Upper*) Tuj1^{+} neuronal projections into the organ of Corti are shown in gray scale. (*Lower*) Merged images with Sox2 (green) and Myo7a (red) channels are shown. (*B*) Representative optical projections of whole mounts from the apical turn of the cochleae of P29 PlpDTA and control mice showing colabeling of presynaptic ribbons (Ctbp2, green) and postsynaptic glutamate receptors (GluR2, red). (*C*) Quantification of Ctbp2 puncta per IHC at different regions along the organ of Corti tonotopic map at P25 (mean ± SEM, $n = 3$–4). (*D*) Quantification of GluR2 puncta per IHC at different regions along the organ of Corti tonotopic map at P25 (mean ± SEM, $n = 3$). (*E*) Plastic cross-sections of the P25 spiral ganglion (*Upper*) and modiolus (*Lower*) of PlpDTA and control mice. (*F*) ABR thresholds from 7-wk-old PlpDTA and control mice (mean ± SEM, $n = 11$). No statistical difference in ABR thresholds was observed in PlpDTA and control mice. (Scale bars: 10 um.)

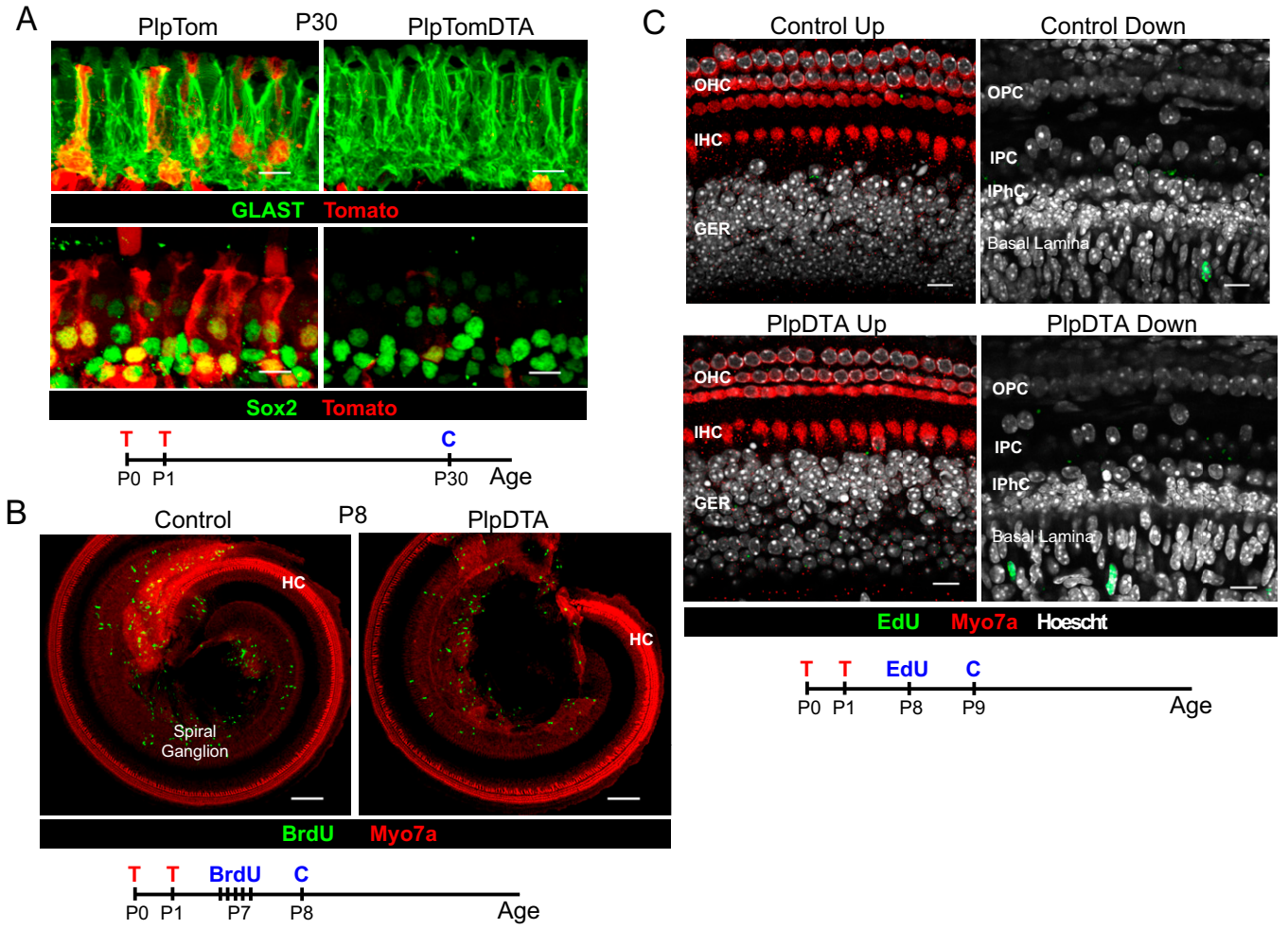

Fig. S4. IBC/IPhC repopulation does not involve clonal expansion of the same population or proliferation within the organ of Corti. (*A*) Representative optical projection of whole mounts from the organ of Corti of PlpTom and PlpTomDTA mice induced with tamoxifen at P0 and P1 and cochleae collected at P30. The timeline below the images shows time points for tamoxifen injection (T) and cochleae collection (C). (*B*) Representative low-resolution images of the apex–middle region of the organ of Corti of PlpDTA and control mice showing the absence of $BrdU^+$ cells (green) in the area close to the HCs ($Myo7a^+$; red) but the presence of $BrdU^+$ cells in the more medial spiral ganglion. At P7, 5 BrdU injections were administered at 2-h intervals; the timeline of tamoxifen induction and cochleae collection is shown below the images. (*C*) Representative high-resolution images of the middle turn of the organ of Corti of PlpDTA and control mice showing no EdU^+ cells (green) in the area close to the HCs ($Myo7a^+$; red) but a few green cells in the basal lamina medial to the IPhC (Hoechst; nuclei in gray scale). Up, image taken at the level of the HC nuclei; Down, image taken at a lower level in the *z* axis of the epithelium where the PC and IPhC nuclei are located. The timeline of tamoxifen induction, EdU injection, and cochleae collection is shown below the images. (Scale bars: *A* and *C*, 10 μm; *B*, 100 μm.)

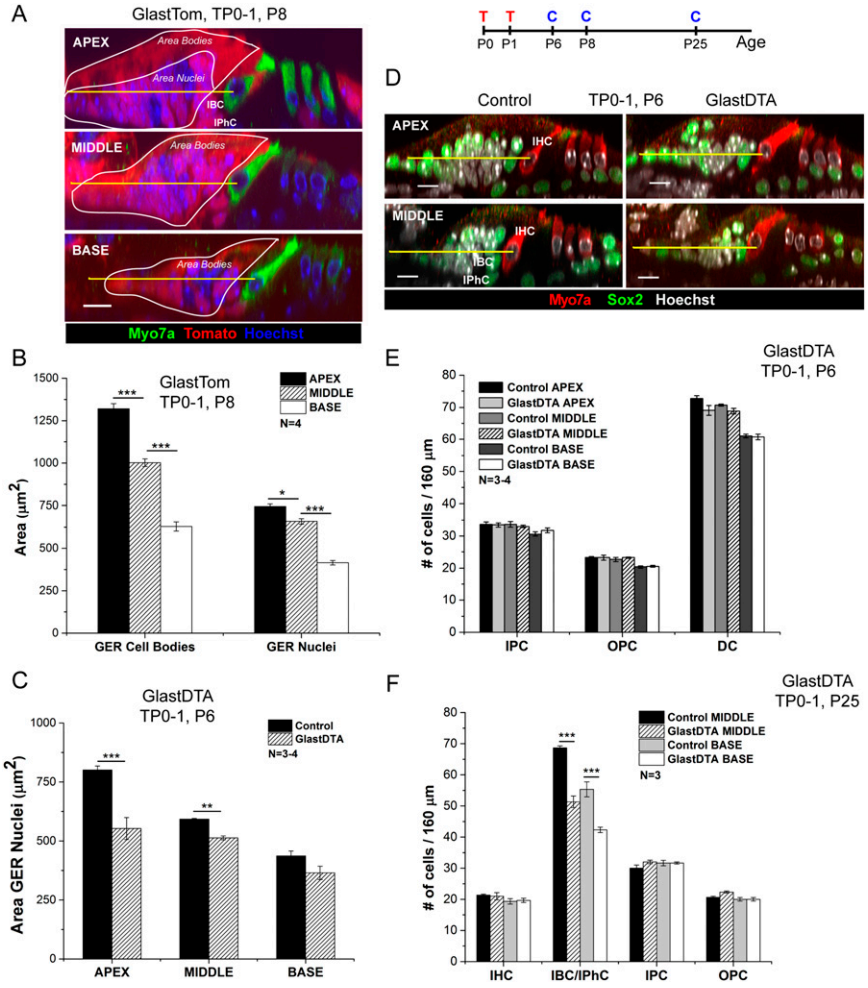

Fig. S5. IBC/IPhC repopulation is affected when GER cells are effectively eliminated in GlastDTA mice treated with tamoxifen at P0 and P1. (*A*) Representative optical cross-sections extracted from *z*-stacks of whole mounts from the apical, middle, and basal turns of the cochleae of GlastTom mice injected with tamoxifen at P0 and P1. Cochleae were collected at P8. Myo7a$^+$ HCs are shown in green, Tomato$^+$ cells are shown in red, and nuclei labeled with Hoechst are shown in blue. The yellow lines mark the 70-μm distance from the IHCs where the GER quantifications shown in *B* were made. White outlines show the limits used to calculate area of the GER occupied by cell bodies or nuclei. The timeline of tamoxifen induction (T) and cochleae collection (C) for analysis is shown at the right. (*B*) Quantification of the areas occupied by cell bodies and nuclei of GER cells in the apical, middle, and basal turns of the cochleae of GlastTom mice at P8 (mean ± SEM, $n = 4$). (*C*) Quantification of the areas occupied by nuclei of GER cells in apical, middle, and basal turns of the cochleae of GlastDTA and control mice at P6 after tamoxifen injection at P0 and P1 (mean ± SEM, $n = 3$–4). (*D*) Representative optical cross-sections extracted from *z*-stacks of whole mounts from the apical and middle turns of the cochleae of GlastDTA and control mice injected with tamoxifen at P0 and P1. Cochleae were collected at P6. Myo7a$^+$ HC are shown in red, Sox2$^+$ cells are shown in green, and nuclei labeled with Hoechst are shown in gray scale. The yellow lines mark the 70-μm distance from the IHCs where GER quantifications shown in *C* were made. (*E*) Quantification of number of Sox2$^+$ PCs and DCs in 160-μm regions of the apical, middle, and basal turns of the cochleae of GlastDTA and control mice injected with tamoxifen at P0 and P1 and samples collected at P6 (mean ± SEM, $n = 3$–4). (*F*) Quantification of number of IHCs and Sox2$^+$ SCs in 160-μm regions of the middle and basal turns of the cochleae of GlastDTA and control mice injected with tamoxifen at P0 and P1; samples were collected at P25 (mean ± SEM, $n = 3$). IBC/IPhC, inner border and inner phalangeal cells; IPC, inner pillar cells; OPC, outer pillar cells. Statistical differences in areas and cell numbers were determine by two-way ANOVA followed by Student *t* test with Bonferroni correction. (Scale bars: 10 μm.) *$P < 0.05$, **$P < 0.01$, ***$P < 0.001$.

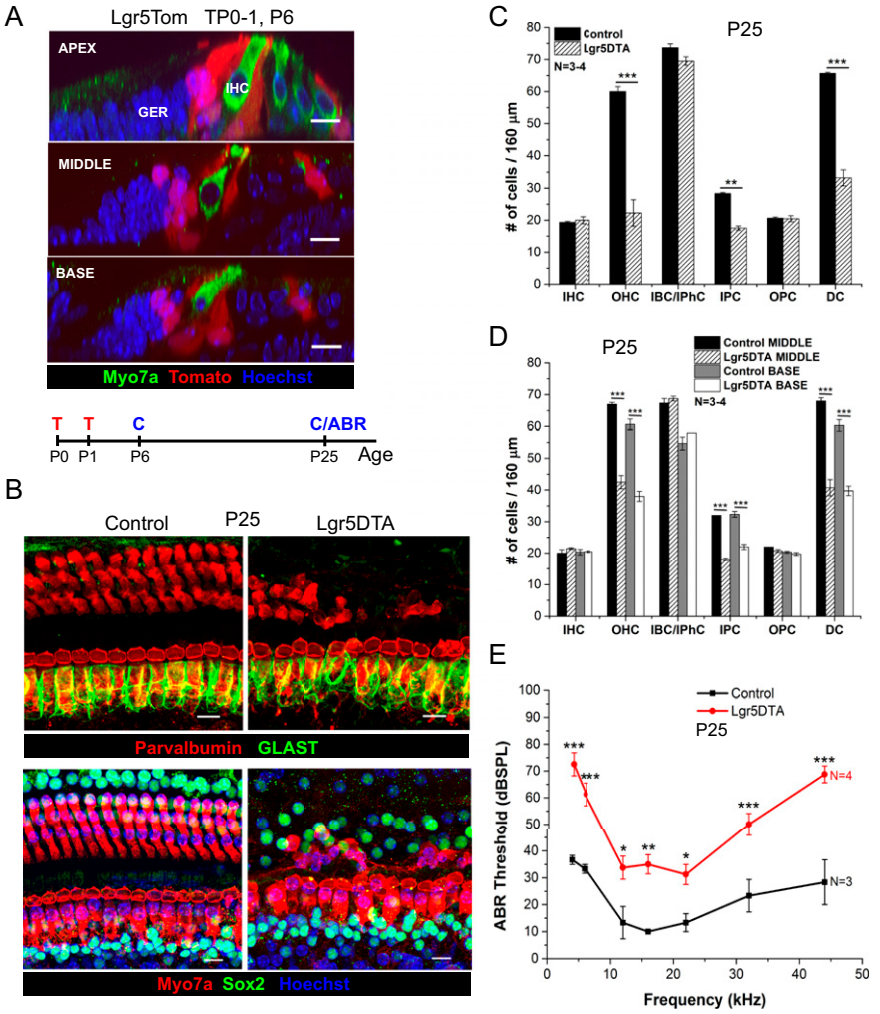

Fig. S6. Lgr5^{+} border cells are not the main source of IBC/IPhC repopulation. (*A*) Representative optical cross-sections extracted from *z*-stacks of whole mounts from the apical, middle, and basal turns of the cochleae of Lgr5Tom mice injected with tamoxifen at P0 and P1. Cochleae were collected at P6. Myo7a^{+} HCs are shown in green, Tomato^{+} cells are shown in red, and nuclei labeled with Hoechst are shown in blue. The timeline of tamoxifen induction (T) and cochleae collection (C) for analysis is shown below the images. (*B*) Representative optical projections of whole mounts from the apical turns of the cochleae of Lgr5DTA and control mice induced with tamoxifen at P0 and P1. Cochleae were collected at P25. (*Upper*) Myo7a^{+} HC are shown in red, and GLAST^{+} IBCs/IPhCs are shown in green. (*Lower*) Myo7a^{+} HC are shown in red, Sox2^{+} SCs are shown in green, and nuclei labeled with Hoechst are shown in blue. (*C* and *D*) The graphs in *C* and *D* are presented separately for clarity. Statistical differences in cell numbers were determined by two-way ANOVA followed by Student *t* test with Bonferroni correction (**$P < 0.01$, ***$P < 0.001$). DC, Deiters' cells; IBC/IPhC, inner border and inner phalangeal cells; IHC, inner hair cells; IPC, inner pillar cells; OHC, outer hair cells; OPC, outer pillar cells. (*C*) Quantification of the number of HCs and Sox2^{+} SCs targeted by Lgr5CreER^{T2} in 160-µm regions of the apical turn of the cochleae of Lgr5DTA and control mice at P25 (mean ± SEM, $n = 3$–4). (*D*) Quantification of the number of HCs and Sox2^{+} SCs targeted by Lgr5CreER^{T2} in 160-µm regions of the middle and basal turns of the cochleae of Lgr5DTA and control mice at P25 (mean ± SEM, $n = 3$–4). (*E*) ABR thresholds measured from Lgr5DTA and control mice at P25 (mean ± SEM, $n = 3$–4). Statistical differences in thresholds at each frequency analyzed (4, 6, 12, 16, 22, 32, and 44 kHz) were determined by two-way ANOVA followed by Student *t* test with Bonferroni correction. (Scale bars: 10 um.) *$P < 0.05$, **$P < 0.01$, ***$P < 0.001$.

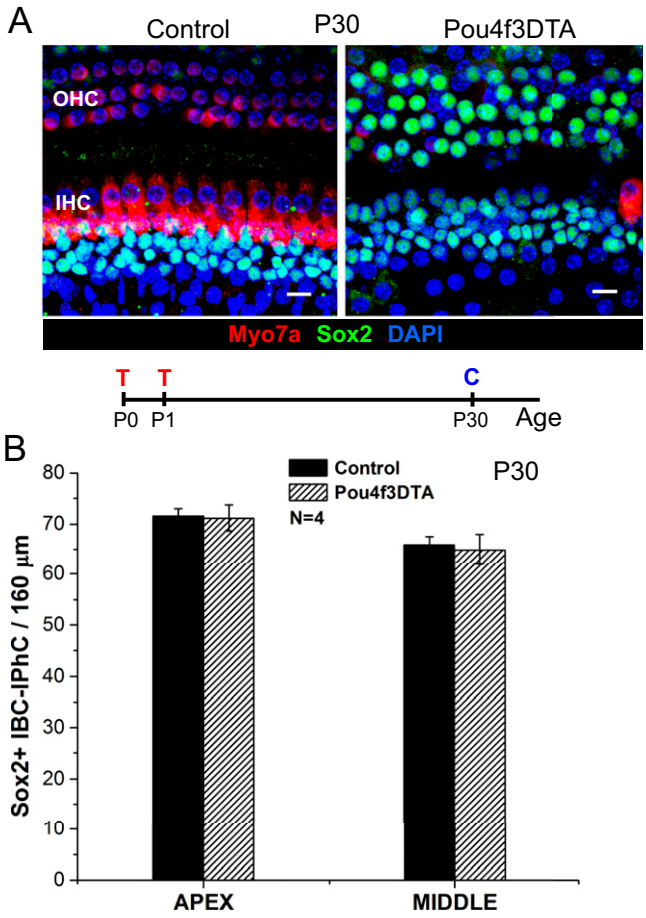

Fig. S7. IBC/IPhC numbers are unaffected after specific ablation of HCs in Pou4f3DTA mice. (*A*) Representative optical sections of whole mounts from the apical turns of the cochleae of Pou4f3DTA and control mice injected with tamoxifen at P0 and P1. Cochleae were collected at P30. Myo7a^{+} HCs are shown in red, Sox2^{+} cells are shown in green, and nuclei labeled with DAPI are shown in blue. The timeline of tamoxifen induction (T) and cochlea collection (C) for analysis is shown below the images. (*B*) Quantification of number of Sox2^{+} IBCs/IPhCs in 160-µm regions of the apical and middle turns of the cochleae of Pou4f3DTA and control mice injected with tamoxifen at P0 and P1. Samples were collected at P30 (mean ± SEM, $n = 4$). No statistical differences in cell numbers are found in Pou4f3DTA and control mice (two-way ANOVA followed by Student *t* test with Bonferroni correction). (Scale bars: 10 um.)

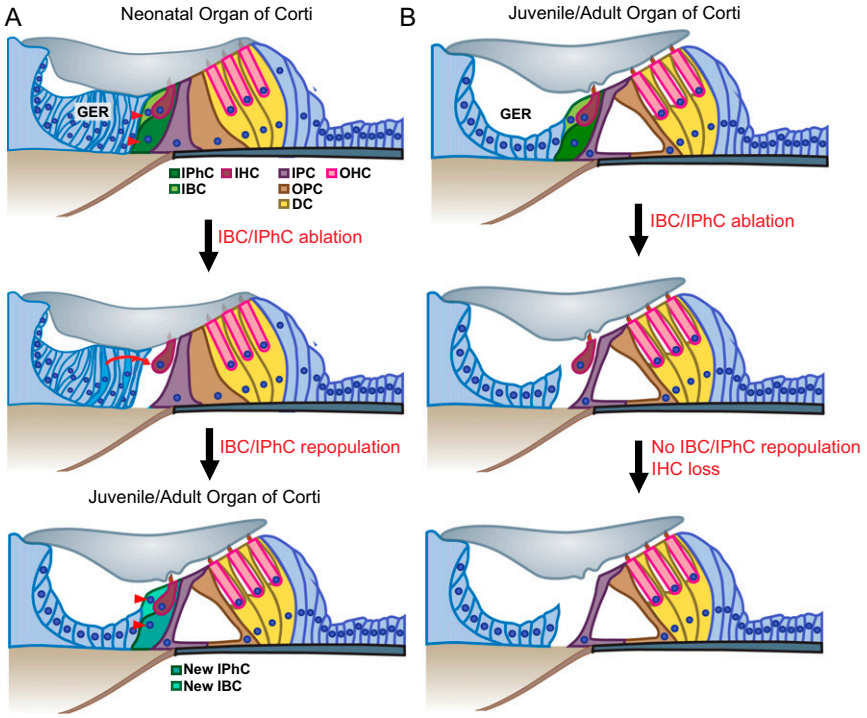

Fig. S8. Proposed mechanism of IBC/IPhC repopulation after postnatal ablation. (*A*) Sequence of events that occur in the organ of Corti after neonatal ablation of IBCs/IPhCs showing cell loss and effective replacement by juvenile/adult ages. The color code for cell types is shown in the top panel. GER cells are highlighted, suggesting that this cell pool may contribute to IBC/IPhC replacement (red arrow in middle panel). Red arrowheads (top and bottom panels) indicate the locations of IBC/IPhC nuclei that differ in PlpDTA and control mice as shown in Fig. 1*G*. (*B*) Sequence of events that occur in the organ of Corti after juvenile or adult ablation of IBCs/IPhCs showing cell loss and absence of replacement in a similar time window (3 wk). This result correlates with the absence of GER cells at juvenile and adult ages. DC, Deiters' cell; GER, greater epithelial ridge; IBC, inner border cell; IHC, inner hair cell; IPC, inner pillar cell; IPhC, inner phalangeal cell; OHC, outer hair cell; OPC, outer pillar cell.